

Journal of Materials Chemistry A

Materials for energy and sustainability

Accepted Manuscript

This article can be cited before page numbers have been issued, to do this please use: Y. Xue, F. Cao, P. Huang, Y. Su and Y. Cheng, *J. Mater. Chem. A*, 2020, DOI: 10.1039/C9TA14040A.



This is an Accepted Manuscript, which has been through the Royal Society of Chemistry peer review process and has been accepted for publication.

Accepted Manuscripts are published online shortly after acceptance, before technical editing, formatting and proof reading. Using this free service, authors can make their results available to the community, in citable form, before we publish the edited article. We will replace this Accepted Manuscript with the edited and formatted Advance Article as soon as it is available.

You can find more information about Accepted Manuscripts in the [Information for Authors](#).

Please note that technical editing may introduce minor changes to the text and/or graphics, which may alter content. The journal's standard [Terms & Conditions](#) and the [Ethical guidelines](#) still apply. In no event shall the Royal Society of Chemistry be held responsible for any errors or omissions in this Accepted Manuscript or any consequences arising from the use of any information it contains.

ARTICLE

Isomeric Effect of Fluorene-based Fused-ring Electron Acceptors to Achieve High-Efficiency Organic Solar Cells

Yung-Jing Xue^a, Fong-Yi Cao^a, Po-Kai Huang^a, Yen-Chen Su^a and Yen-Ju Cheng^{*ab}

Received 00th January 20xx,
Accepted 00th January 20xx

DOI: 10.1039/x0xx00000x

Acceptor-donor-acceptor (A-D-A) non-fullerene electron acceptors (NFEAs) using ladder-type donor structures have become the dominant n-type materials for achieving high-efficiency OSCs. In this work, two isomeric fluorene-based ladder-type structures FCTT (TT-C-F-C-TT) and FTCT (T-C-TFT-C-T) have been designed and synthesized. These two isomeric donors with the different fused-ring arrangement, molecular geometry, and side-chain placement were end-capped with the FIC acceptors to form two NFEAs FCTT-FIC and FTCT-FIC isomeric materials. Compared to FTCT-FIC using the thiophene (T)-terminal donor, FCTT-FIC with the thienothiophene (TT)-terminal donor has more evenly-distributed side chains among the backbone and less steric hindrance near the FIC acceptors, which enables stronger antiparallel π - π packing among the end-groups to create a channel for efficient electron transport, as evidenced by the thin-film GIWAXS measurements. FCTT-FIC displayed a larger optical bandgap and deeper-lying energy levels than its FTCT-FIC isomer. Compared to the PBDB-T:FTCT-FIC device, the PBDB-T:FCTT-FIC device showed a higher PCE of 10.32% with enhanced J_{sc} of 19.63 mA cm⁻² and FF of 69.14%. PM6:FCTT-FIC device using PM6 as a p-type polymer achieved a highest PCE of 12.23%. By introducing PC₇₁BM as the second acceptor to enhance the absorption at shorter wavelengths, optimize the morphology and facilitate electron transport, the ternary-blend PM6:FCTT-FIC:PC₇₁BM (1:1:0.5 in wt%) device yielded the highest PCE of 13.37% with a V_{oc} of 0.92 V, a higher J_{sc} of 19.86 mA cm⁻², and an FF of 73.2%. This result demonstrated that the TT-terminal ladder-type donor is generally a better molecular design than the corresponding T-terminal ladder-type isomer for the development of new A-D-A NFEAs.

1. Introduction

Organic solar cells (OSCs) have been considered as the promising candidates for the next generation solar energy converter due to their intrinsic properties of lightweight, flexibility, semi-transparency at visible region and solution-process availability.¹⁻¹³ In the past few years, n-type non-fullerene acceptors (NFEAs) have been rapidly developed for achieving high efficiency OSCs.¹⁴⁻⁴¹ The organic-based NFEAs can possess strong absorption covering UV-visible and near infrared regions and tunable HOMO/LUMO energy levels to simultaneously achieve higher short-circuit current density (J_{sc}) and open-circuit voltage (V_{oc}).³³⁻³⁵ The current state-of-the-art FREAs are based on an A-D-A (acceptor-donor-acceptor) architecture consisting of a central electron-rich donor (D) end-capped by two electron-deficient acceptors (A). The push-pull D-A system can induce intramolecular charge transfer for strong light-harvesting ability. The electronic and steric properties of A-D-A NFEAs can be optimized by independently modifying the central electron-rich donors (D)^{18, 23, 29, 42-49}, end-group electron-

deficient acceptors (A)^{32, 50-55} and solubilizing aliphatic side-chains^{27, 56-58}. The central donor core particularly plays a more important role in determining the intrinsic characteristics of NFEAs. The mainstream design of the central symmetrical donor unit is based on the concept of molecular rigidification and planarization.⁵⁹⁻⁶⁹ Incorporation of sp³-carbon bridges to covalently ring-lock adjacent electron-rich aryl groups leads to a fully planarized ladder-type structure which can elongate effective conjugation, improve charge mobility and promote intermolecular interactions.⁶⁸⁻⁷⁰ Moreover, alkyl side-chains attached on the central ladder-type donor are also crucial for tailoring intermolecular interactions between the N-type NFEA molecules. It is generally believed that A-D-A type NFEAs tend to self-assemble through the antiparallel stacking of the acceptor end-groups that generate a channel for electron transport.⁶¹ The function of side-chains should prevent severe aggregation for solution processibility without interrupting the antiparallel packing among end-groups.⁷¹ As a result, the location of the side-chains should keep distance with the acceptor end-groups. Various fascinating ladder-type structures have been developed and utilized for making high-performance A-D-A NFEAs. These lengthy conjugated ladder-type donors, mostly comprised of thiophene (T), benzene (B) and embedded di(4-hexylphenyl) cyclopentadienyl (C) moieties, can have several structural isomers. Investigation of isomeric ladder-type

^a Department of Applied Chemistry, National Chiao Tung University, 1001 University Road, Hsinchu, Taiwan 30010.

^b Center for Emergent Functional Matter Science, National Chiao Tung University, 1001 University Road, Hsinchu, Taiwan 30010.

† Footnotes relating to the title and/or authors should appear here.

Electronic Supplementary Information (ESI) available: [details of any supplementary information available should be included here]. See DOI: 10.1039/x0xx00000x

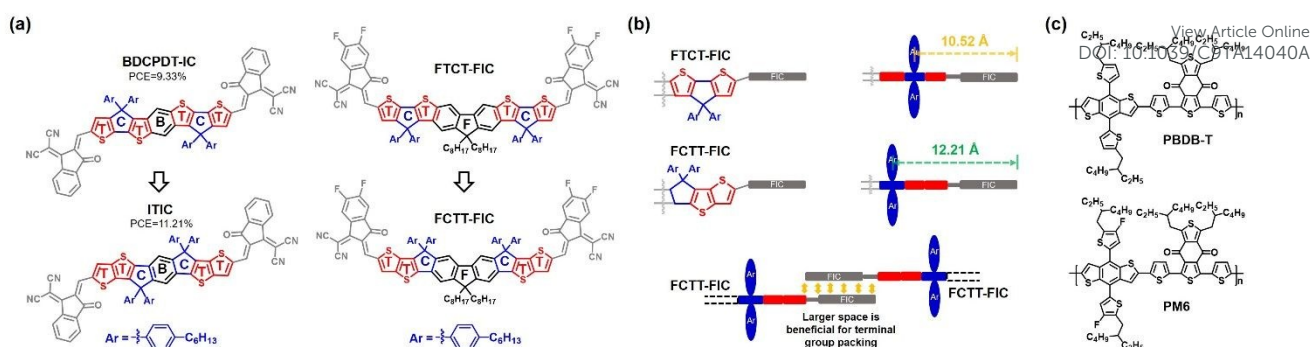


Fig 1. Chemical structures of (a) BDCPDT-IC, ITIC, FTCT-FIC and FCTT-FIC; (b) the diagram of the antiparallel stacking of the terminal FIC moieties. (c) chemical structures of PBDB-T and PM6. Polymer structures PBDBT and PM6.

structures with different main-chain and side-chain arrangements is very appealing and promising for developing new NFEAs. In 2015, Zhan et al first reported a high-performance A-D-A type ITIC utilizing a IC (1,1-dicyanomethylene-3-indanone) acceptor and a ladder-type IDTT (Fig 1a) donor which contains a central benzene ring (B), two outer thienothiophenes (TT) and two embedded Cs (symbolized as TT-C-B-C-TT).²³ By shifting the two outer thiophenes in TT-C-B-C-TT to the inner part, an isomeric structure T-C-TBT-C-T (also named as BDCPDT) was designed and synthesized (Fig 1a). The corresponding non-fullerene acceptor BDCPDT-IC was thus prepared.³¹ The ITIC-based devices generally exhibited better device performance in comparison with the BDCPDT-IC-based devices. This result implied that using TT-terminal ladder-type structure seems to be a more superior design compared to its corresponding T-terminal isomer. Furthermore, Zhan et al. designed two isomeric ladder-type NFEAs, FNIC1 and FNIC2.⁷² It is interesting to find that TT-terminal FNIC2 also showed better device performance than T-terminal FNIC1.

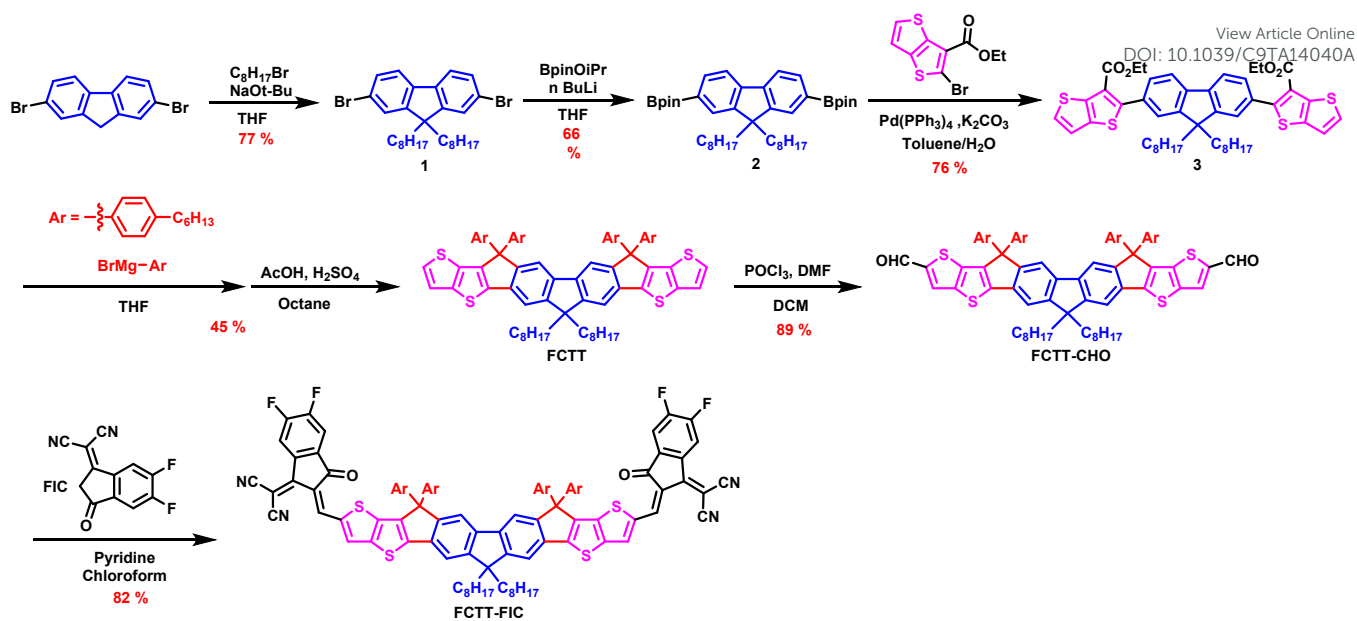
It is of great interest to systematically compare TT-terminal and T-terminal isomeric NFEAs. We recently developed another NFEA denoted as FTCT-FIC using a fluorene-based nonacyclic ladder-type core FTCT (Fig 1a).⁶⁹ FTCT (can also be symbolized as T-C-TFT-C-T) contains a central dithienofluorene (TFT), two outer thiophenes and two embedded Cs. FTCT-FIC has strong absorption in the visible and near-infrared regions but weak crystallinity. The device with PBDB-T:FTCT-FIC (1:1.5 in wt%) showed a decent PCE of 9.58% with a V_{oc} of 0.86 V, a J_{sc} of 19.01 mA cm^{-2} , and an FF of 58.61%. The low FF was attributed to the improper morphology and lower electron mobility. It needs to be pointed out that all the side chains in FTCT are situated at the same side of the conjugated backbone, which might not be ideal for molecular packing. Meanwhile, the geminal di(4-hexylphenyl) groups on the sp^3 -carbon of the cyclopentadienyl (CP) ring are also close to the FIC end-groups (ca. 10.52 Å), which exerts certain steric hindrance to attenuate end-group packing (Fig 1b).

In this research, we further synthesized another isomeric TT-terminal fluorenedicyclopentathieno[3,2-b]thiophene FCTT (also structurally symbolized as TT-C-F-C-TT) and its

corresponding FCTT-FIC (Fig 1b) FREA. By shifting the inner thiophenes in FTCT to the terminal part, the aliphatic side-chains are more evenly distributed at the both sides of FCTT backbone. Meanwhile, the distance between the side-chains on CP rings and the FIC end-groups also becomes longer (ca. 12.21 Å). FCTT-FIC displayed larger optical bandgap and deeper HOMO/LUMO energy levels compared with its FTCT-FIC isomer. Compared to the PBDB-T:FTCT-FIC-based device, the device using PBDB-T:FCTT-FIC showed a higher PCE of 10.32%. Furthermore, the PM6:FCTT-FIC-based device exhibited dramatically improved efficiency of 12.23%. The chemical structures of PBDB-T and PM6 are shown in Fig 1c. By introducing PC₇₁BM as the third component to enhance the absorption at shorter wavelengths, optimize the morphology and facilitate electron transport,⁷³⁻⁷⁷ the ternary-blend device using PM6:FCTT-FIC:PC₇₁BM (1:1:0.5 in wt%) yielded a highest PCE of 13.37% with a V_{oc} of 0.92 V, a higher J_{sc} of 19.86 mA cm^{-2} , and an FF of 73.2%.

2. Results and discussion

The synthetic route of FCTT-FIC is depicted in **Scheme 1**. 2,7-dibromo-9H-fluorene was reacted with 1-bromooctane under basic conditions to form compound **1** in 77% yield. Compound **1** was lithiated and then reacted with 2-isopropoxy-4,4,5,5-tetramethyl-1,3,2-dioxaborolane to yield compound **2** in 66% yield. Suzuki coupling of compound **2** with ethyl 2-bromothieno[3,2-b]thiophene-3-carboxylate afforded compound **3** in 76% yield. Reaction of **3** with 4-hexylphenylmagnesium bromide followed by acid-catalyzed cyclization resulted in the formation of FCTT in an overall 45% yield. The formylation of FCTT generated FCTT-CHO in 89% yield. Condensation of FCTT-CHO with 1,1-dicyanomethylene-5,6-difluoro-3-indanone (FIC) afforded the product of FCTT-FIC. FCTT-FIC showed good solubility in common organic solvents such as chloroform and chlorobenzene. The detailed synthetic procedure, mass spectrometry, ¹H NMR and ¹³C NMR of new compounds are shown in supporting information. FCTT-FIC exhibited a decomposition temperature (Td) at 339 °C in the thermogravimetric analysis (TGA) measurement, showing good thermal stability. In the differential scanning calorimetry (DSC) measurement, FCTT-FIC did not show melting point and



Scheme 1. Synthesis of FCTT-FIC.

crystallization transition. The normalized absorption spectra of PM6, PBDB-T, FTCT-FIC and FCTT-FIC in chlorobenzene solution and thin film are shown in Fig 2a and their intrinsic properties are listed in Table 1. In solution state, FCTT-FIC displayed strong absorption in 500-750 nm region with a high extinction coefficient of $1.38 \times 10^5 \text{ M}^{-1} \text{ cm}^{-1}$ at the λ_{max} of 675 nm. The λ_{max} of FCTT-FIC was significantly red-shifted by 34 nm in thin film, indicating the strong intermolecular interactions in the solid state. The optical bandgap of FCTT-FIC was estimated to be 1.53 eV. The cyclic voltammogram (CV) and the energy levels of FCTT-FIC are shown in Fig S2 and Fig 2b, respectively. The highest occupied molecular orbital (HOMO) and lowest unoccupied molecular orbital (LUMO) of FCTT-FIC were estimated to be $-5.56/-4.03$ eV. Compared to FTCT-FIC, FCTT-FIC showed hypsochromically shifted absorption and deeper-lying energy levels, indicating that rearrangement of the conjugation leads to the alteration of electronic properties.

31G(d,p) level. FTCT-FIC and FCTT-FIC with the simplified side-chain (the octyl and 4-hexylphenyl groups are simplified to ethyl and 4-methylphenyl groups, respectively) are used for simulation. The optimal geometries of the simplified FTCT-FIC and FCTT-FIC structures are displayed in Fig 3. Both FTCT-FIC and FCTT-FIC possessed highly planar conjugated backbone. Furthermore, the distance between the center of the alkylphenyl side-chains and the edge of the FIC was calculated. FCTT-FIC showed a longer distance of 12.21 Å than FTCT-FIC (10.52 Å), which can reduce the steric repulsion and allow more space for intermolecular antiparallel stacking of the terminal FIC moieties. The dipole moment of the half FTCT-FIC and FCTT-FIC molecules were also estimated to be 9.39 D and 9.66 D, respectively. The larger dipole moments strengthen donor-acceptor communication leading to the strong intramolecular charge transfer and red-shifted absorption spectra.

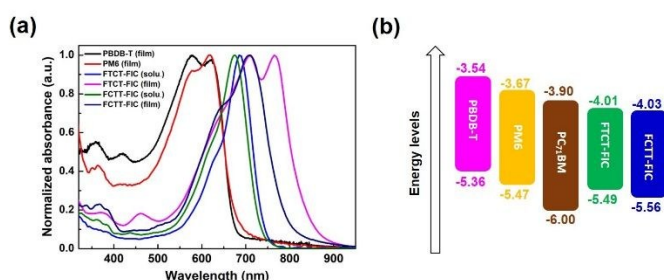


Fig 2. (a) UV-vis absorption spectra of PBDB-T, PM6, FTCT-FIC and FCTT-FIC in chlorobenzene solution and thin film, (b) energy levels of PBDB-T, PM6, PC₇₁BM, FTCT-FIC and FCTT-FIC estimated by cyclic voltammetry.

To gain the understanding of the differences on the backbone conformation and the dipole moment of the molecule, we applied the density functional theory (DFT) calculations with the Gaussian09 suite15 at the B3LYP/6-

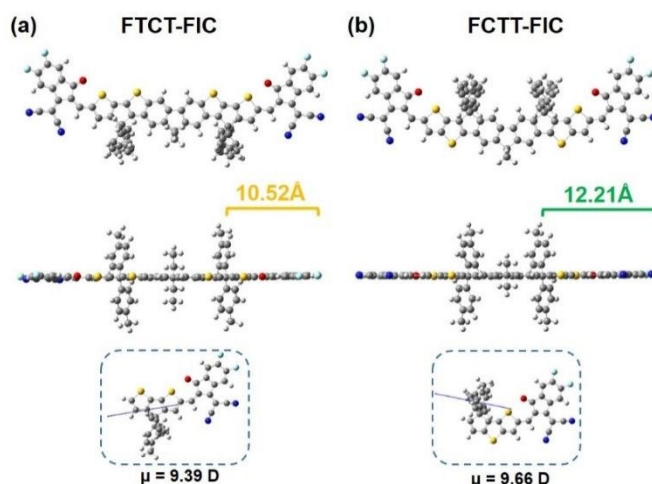


Fig 3. Top/side view of the DFT optimized conformation and the dipole moment of half molecule of (a) FTCT-FIC and (b) FCTT-FIC.

Table 1. Summary of the intrinsic properties of FTCT-FIC and FCTT-FIC.

FREA	Extinction coefficient ($\times 10^5 \text{ cm}^{-1}\text{M}^{-1}$) ^a	λ_{max} (nm)		λ_{onset} (nm) ^b	$E_{\text{g}}^{\text{opt}}$ (eV) ^c	HOMO (eV) ^d	LUMO (eV) ^d	$E_{\text{g}}^{\text{ele}}$ (eV) ^d
		CB	Film					
FTCT-FIC	1.80	688	766	849	1.46	-5.49	-4.01	1.48
FCTT-FIC	1.38	675	709	799	1.55	-5.56	-4.03	1.53

^acalculated at λ_{max} . ^bcalculated in the solid state, ^c $E_{\text{g}}^{\text{opt}} = 1240/\lambda_{\text{onset}}$, ^ddetermined by cyclic voltammetry.

Table 2. Characteristics of the devices with ITO/ZnO/active layer/MoO₃/Ag.

Blend system	Blend ratio in wt%	V_{oc} (V)	J_{sc} (mA cm ⁻²)	FF (%)	PCE (%)	μ_{hole} (cm ² V ⁻¹ s ⁻¹)	μ_{ele} (cm ² V ⁻¹ s ⁻¹)
PBDB-T: FTCT-FIC	1:1.5	0.86 (0.86±0)	19.01 (19.19±0.29)	58.61 (57.83±0.88)	9.58 (9.54±0.02)	1.03×10^{-5}	4.13×10^{-6}
PBDB-T: FCTT-FIC	1:1	0.76 (0.76±0)	19.63 (19.88±0.60)	69.14 (66.43±1.81)	10.32 (10.03±0.18)	2.81×10^{-5}	1.10×10^{-4}
PM6:FCTT-FIC	1:1	0.90 (0.9±0.01)	19.49 (19.36±0.77)	69.73 (69.24±1.75)	12.23 (12.01±0.24)	4.71×10^{-6}	2.50×10^{-5}
PM6:FCTT-FIC: PC ₇₁ BM	1:1:0.5	0.92 (0.92±0)	19.86 (20.12±1.03)	73.20 (70.97±1.85)	13.37 (13.12±0.43)	2.32×10^{-5}	3.03×10^{-5}
	1:1:1	0.92 (0.92±0.01)	18.48 (18.39±0.32)	72.71 (71.01±0.99)	12.36 (12.03±0.14)	6.96×10^{-6}	1.02×10^{-5}
	1:1:1.5	0.92 (0.92±0)	17.83 (17.75±0.31)	71.48 (70.62±1.78)	11.72 (11.53±0.16)	6.25×10^{-6}	1.17×10^{-5}

The average values with standard deviation over 10 cells are shown in parenthesis.

To investigate the photovoltaic characteristics, the inverted OSC devices with the configuration of ITO/ZnO/Active layer/MoO₃/Ag were fabricated. Characteristics of the devices, the J-V curves and the external quantum efficiency (EQE) spectra are shown in Table 2 and Fig 4. The medium-bandgap PBDBT having the suitable energy level alignment and complementary absorption spectrum was used to blend with FTCT-FIC and FCTT-FIC. The optimized device using PBDB-T:FTCT-FIC (1:1.5 in wt%) exhibited a PCE of 9.58% with a V_{oc} of 0.86 V, a J_{sc} of 19.01 mA cm⁻², and an FF of 58.61%, while the optimized device with PBDB-T:FCTT-FIC (1:1 in wt%) exhibited a higher PCE of 10.32% with a V_{oc} of 0.76 V, a J_{sc} of 19.63 mA cm⁻², and an FF of 69.14%. The lower V_{oc} of the PBDB-T:FCTT-FIC device is associated with the deeper-lying LUMO level of FCTT-FIC. The discrepancy of V_{oc} value can be ascribed to the difference of blending ratios and morphology. It is notable that the device with PBDB-T:FCTT-FIC showed much higher FF than

that of the PBDB-T:FTCT-FIC, indicating that the PBDB-T:FCTT-FIC system possessed better charge transport and negligible charge recombination. To deeply explore the charge transport, the hole-only devices (ITO/PEDOT:PSS/active layer/Au) and electron-only devices (Al/active layer/Al) were fabricated to evaluate the hole and electron mobility by space-charge limit current (SCLC) model (Fig S2). The hole and electron mobilities were estimated to be $1.03 \times 10^{-5}/4.13 \times 10^{-6}$ for PBDB-T:FTCT-FIC blend and $2.81 \times 10^{-5}/1.1 \times 10^{-4}$ cm²V⁻¹s⁻¹ for PBDB-T:FCTT-FIC blend. It is envisaged that FCTT-FIC with the side-chains at the more inner position is beneficial for the end-group stacking. Therefore, PBDB-T:FCTT-FIC blend displayed higher hole and electron mobilities leading to the improved J_{sc} and FF. It is known that precise energy level alignment between a p-type material and an n-type FREA can ensure the efficient charge separation and minimize photon energy loss (E_{loss}) to enhance the V_{oc} . E_{loss} is correlated to the potential energy

difference between the absorbed photon and the released electron.^{78,79} PM6 with the similar absorption spectrum but lower-lying HOMO/LUMO levels was used to blend with FCTT-FIC as the p-type material. Compared to the device with PBDB-T:FCTT-FIC, the PM6:FCTT-FIC (1:1 in wt%) device showed an increased PCE of 12.23% and the V_{oc} significantly enhanced from 0.76 V to 0.90 V. Furthermore, we calculated the E_{loss} of the devices based on the equation of $E_{loss} = E_g^{opt} - eV_{oc}$ where the E_g^{opt} is the lowest optical bandgap among the donor and acceptor components. The E_{loss} of the PBDB-T:FCTT-FIC and PM6:FCTT-FIC devices are estimated to be 0.77 eV and 0.63 eV, respectively. The lower E_{loss} of the PM6:FCTT-FIC device is associated with the smaller HOMO level difference between the PM6 and FCTT-FIC.

Ternary-blend system incorporating a fullerene derivative and an FREA has been widely used to achieve high-performance OSCs. We introduced the PC₇₁BM as the second N-type material to form a ternary-blend PM6:FCTT-FIC:PC₇₁BM with different blending ratios. The PM6:FCTT-FIC:PC₇₁BM (1:1:0.5 in wt%) device showed the best PCE of 13.37% with the highest J_{sc} of 19.86 mA cm⁻² and FF of 73.2%. The increased J_{sc} was attributed to the enhanced EQE from 400 nm to 500 nm. Furthermore, all the ternary-blend devices showed the increased V_{oc} of 0.92 V due to the higher-lying LUMO level of PC₇₁BM. When the PC₇₁BM ratio further increased to 1:1:1 and 1:1:1.5 in wt%, the efficiency slightly decreased to 12.36% and 11.72%.

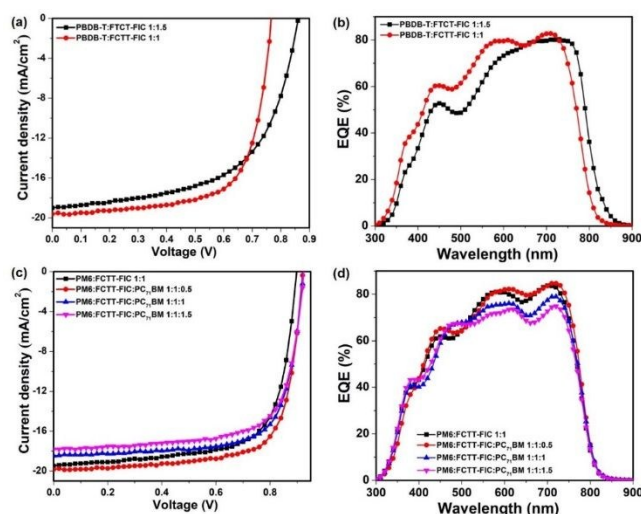


Fig 4. (a) J - V curves and (b) EQE spectra of the devices with PBDB-T:FCTT-FIC (1:1.5 in wt%) and PBDB-T:FCTT-FIC (1:1 in wt%). (c) J - V curves and (d) EQE spectra of the devices with PM6:FCTT-FIC:PC₇₁BM in the ratio of 1:1:0, 1:1:0.5, 1:1:1 and 1:1:1.5 in wt%.

Based on the SCLC mobility results, all the ternary-blend devices exhibited more balance charge transport with the hole/electron mobility ratio of 0.77 (PM6:FCTT-FIC:PC₇₁BM =1:1:0.5), 0.68 (PM6:FCTT-FIC:PC₇₁BM =1:1:1) and 0.53 (PM6:FCTT-FIC:PC₇₁BM =1:1:1.5), respectively, than the binary device (PBDB-T:FCTT-FIC =1:1) with the ratio of 0.19. The more balance charge transport also reflected on the increased FF of the ternary-blend devices. Two-dimensional grazing-incidence wide-angle X-ray diffraction (GIWAXS) was used to study the molecular packing of the pure FREAs and blend films. As shown

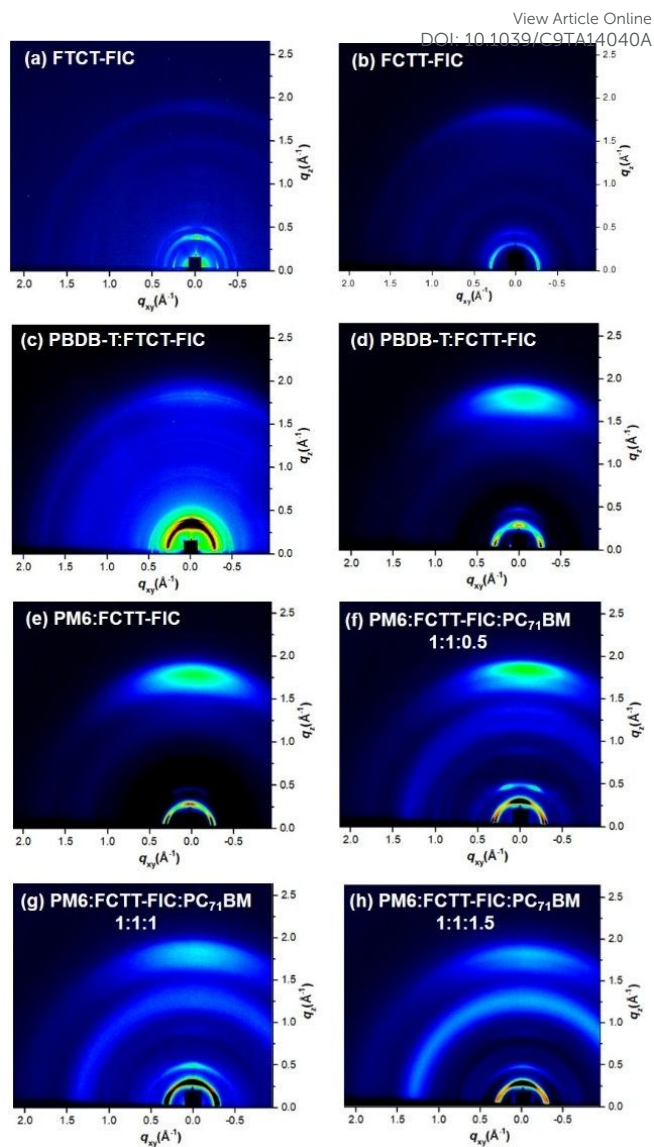


Fig 5. 2-Dimensional GIWAXS images of the films with (a) pure FTCT-FIC, (b) pure FCTT-FIC, (c) PBDB-T:FTCT-FIC, (d) PBDB-T:FCTT-FIC, (e) PM6:FCTT-FIC and PM6:FCTT-FIC:PC₇₁BM with blending ratio (f) 1:1:0.5, (g) 1:1:1 and (h) 1:1:1.5 in wt% films.

in the Fig 5, the pure FTCT-FIC displayed a weak (010) π - π stacking diffraction in the out-of-plane direction with a $q_z = 1.83$ Å⁻¹ corresponding to a π - π distance (d_{π}) of ca. 3.43 Å. On the other hand, the pure FCTT-FIC showed a stronger π - π stacking diffraction at $q_z = 1.82$ Å⁻¹ with a d_{π} of ca. 3.45 Å, indicating that FCTT-FIC possesses stronger face-on stacking interactions.

In the blend films, PBDB-T:FTCT-FIC showed the face-on orientation with the π - π diffraction at $q_z = 1.82$ Å⁻¹ and a d_{π} of ca. 3.46 Å. In addition, PBDB-T:FCTT-FIC revealed two merged π - π diffractions at $q_z = 1.74$ Å⁻¹ and $q_z = 1.84$ Å⁻¹ with the corresponding d_{π} of ca. 3.61 Å and 3.42 Å which can be ascribed to the crystalline PBDB-T and FCTT-FIC domains, respectively. The shorter d_{π} of FCTT-FIC in the PBDB-T:FCTT-FIC blend indicated that PBDB-T induced more compact packing of FCTT-FIC which is beneficial to the electron transport. The face-on orientations of the both PBDB-T and FCTT-FIC crystallines can facilitate the hole and electron transport which is consistent

with the mobility results. The PM6:FCTT-FIC blend presented similar diffraction patterns with PBDB-T:FCTT-FIC, showing face-on π - π stacking signals at $q_z = 1.76 \text{ \AA}^{-1}$ and $q_z = 1.84 \text{ \AA}^{-1}$ with a $d\pi$ of ca. 3.57 \AA and 3.42 \AA from PM6 and FCTT-FIC, respectively. When adding 0.5 wt% of PC₇₁BM into the PM6:FCTT-FIC blend, the 2D pattern showed two more obvious separated π - π diffractions at $q_z = 1.73 \text{ \AA}^{-1}$ and $q_z = 1.87 \text{ \AA}^{-1}$ with a $d\pi$ of ca. 3.64 \AA and 3.35 \AA , suggesting that PC₇₁BM slightly enlarged the d_π of PM6 and tightened the $d\pi$ of FCTT-FIC molecules.

The fine-tuning of the molecular packing by PC₇₁BM effectively adjusted the hole and electron mobilities to yield more balanced charge transport, thus improving J_{sc} and FF in the PM6:FCTT-FIC:PC₇₁BM (1:1:0.5 in wt%) device. However, when the amount of PC₇₁BM increased to 1 and 1.5 weight ratio to PM6, the 2D patterns showed the decreased diffraction intensity of the π - π stacking, leading to the lower charge mobility, J_{sc} and FF. The GIWAXS results are fully consistent with the device performance. Furthermore, the 1-dimensional in-plane and out-of-plane GIWAXS patterns of the films are shown in Fig S4.

To investigate the surface morphology of the blend films, atomic force microscopy (AFM) was used to measure the topography images of the blend system. As shown in the Fig 6, the surface roughness of PBDB-T:FTCT-FIC film is 5.91 nm, while the surface roughness of PBDB-T:FCTT-FIC film greatly decreased to 0.97 nm. The much smooth surface of PBDB-T:FCTT-FIC indicates the improved miscibility between the donor and acceptor, thus enhancing the interfacial contact and facilitating the carrier transport in the device. For the PM6-based blend systems, the surface roughness of PM6:FCTT-FIC film is 3.39 nm, and the ternary-blend PM6:FCTT-FIC:PC₇₁BM (1:1:0.5 in wt%) revealed a much smoother surface with roughness of 1.79 nm, indicating that the introduction of PC₇₁BM formed the better morphology and surface contact.

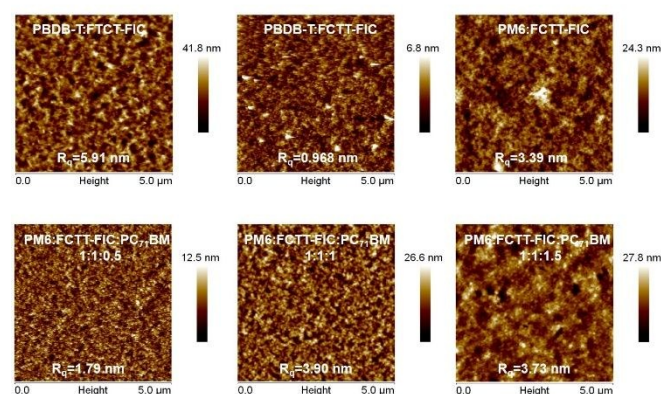


Fig 6. Atomic force microscopy images and the roughness of the PBDB-T:FCTT-FIC:PC₇₁BM blend films with the ratio of (a) 1:1:0, (b) 1:1:0.5, (c) 1:1:1 and (d) 1:1:1.5 in wt%.

3. Conclusions

In summary, the A-D-A nonfullerene materials based on a ladder-type donor have merged as a new generation N-type

materials. Development of new isomeric structures of the state-of-the-art central ladder-type donors provides a straightforward and promising way to effectively optimize the solar cell characteristics. A ladder-type fluorine-based thienothiophene-terminal FCTT (TT-C-F-C-TT), which is an isomeric structure of thiophene-terminal FTCT (T-C-TFT-C-T), was designed and synthesized. The two donors were end-capped with FIC acceptors to form FCTT-FIC and FTCT-FIC FREAs. Considering the electronic effect, FCTT-FIC exhibited a larger optical bandgap and deeper-lying energy levels than FTCT-FIC. The steric effect plays a more important role in determining molecular interactions and packing. The distance between geminal di(4-hexylphenyl) side-chains and the FIC acceptor edge is estimated to be 12.21 \AA for FCTT-FIC using the TT-terminal donor and 10.52 \AA for FTCT-FIC with the T-terminal donor. The longer distance provides more space for the antiparallel packing among the end-groups. As a result, FCTT-FIC exhibited stronger face-on π - π stacking in the both neat film and blend films. The PBDB-T:FCTT-FIC device displayed a higher PCE of 10.32%, an enhanced J_{sc} of 19.63 mA cm^{-2} and an FF of 69.14%, compared to the PBDB-T:FTCT-FIC device. Furthermore, the PM6:FCTT-FIC device can further improve the efficiency to 12.23%. By introducing PC₇₁BM as the third component, the ternary-blend PM6:FCTT-FIC:PC₇₁BM device (1:1:0.5 in wt%) yielded the highest PCE of 13.37% with a V_{oc} of 0.92 V, a higher J_{sc} of 19.86 mA cm^{-2} , and an FF of 73.2%. This research demonstrated that TT-terminal ladder-type structure is a superior donor design for high-performance A-D-A FREAs.

Conflicts of interest

There are no conflicts to declare.

Author information

Author Contributions

Y-C Xue and F-Y Cao are equally contributed to this work.

Acknowledgements

This work is supported by Ministry of Science and Technology, Taiwan (grant No. MOST107-3017-F009-003) and Ministry of Education, Taiwan (SPROUT Project-Center for Emergent Functional Matter Science of National Chiao Tung University). We thank the National Synchrotron Radiation Research Center (NSRRC), and Dr. U-Ser Jeng and Dr. Chun-Jen Su at BL23A1 station.

References

- 1 J. Chen and Y. Cao, *Acc. Chem. Res.* **2009**, *42*, 1709–1718.
- 2 Y. Li, *Acc. Chem. Res.* **2012**, *45*, 723–733.
- 3 Y. Li and Y. Zou, *Adv. Mater.* **2008**, *20*, 2952–2958.
- 4 B. C. Thompson and J. M. Fréchet, *Angew. Chem. Int. Ed.* **2008**, *47*, 58–77.
- 5 A. C. Arias, J. D. MacKenzie, I. McCulloch, J. Rivnay and A. Salleo, *Chem. Rev.* **2010**, *110*, 3–24.

- 6 Y.-J. Cheng, S.-H. Yang and C.-S. Hsu, *Chem. Rev.* **2009**, *109*, 5868–5923.
- 7 S. Günes, H. Neugebauer and N. S. Sariciftci, *Chem. Rev.* **2007**, *107*, 1324–1338.
- 8 C. Duan, F. Huang and Y. Cao, *J. Mater. Chem.* **2012**, *22*, 10416–10434.
- 9 F. He and L. Yu, *J. Phys. Chem. Lett.* **2011**, *2*, 3102–3113.
- 10 H. Zhou, L. Yang and W. You, *Macromolecules* **2012**, *45*, 607–632.
- 11 G. Li, R. Zhu and Y. Yang, *Nat. Photonics* **2012**, *6*, 153–161.
- 12 L. Huo and J. Hou, *Poly. Chem.* **2011**, *2*, 2453–2461.
- 13 G. Yu, J. Gao, J. C. Hummelen, F. Wudl and A. J. Heeger, *Science* **1995**, *270*, 1789–1791.
- 14 C. Yan, S. Barlow, Z. Wang, H. Yan, A. K.-Y. Jen, S. R. Marder and X. Zhan, *Rev. Mater.* **2018**, *3*, 18003.
- 15 P. Cheng, G. Li, X. Zhan and Y. Yang, *Nat. Photonics* **2018**, *12*, 131–142.
- 16 H. Kang, W. Lee, J. Oh, T. Kim, C. Lee and B. J. Kim, *Acc. Chem. Res.* **2016**, *49*, 2424–2434.
- 17 T. Kim, J.-H. Kim, T. E. Kang, C. Lee, H. Kang, M. Shin, C. Wang, B. Ma, U. Jeong, T.-S. Kim and B. J. Kim, *Nat. Commun.* **2015**, *6*, 8547–8553.
- 18 Y. Lin, Q. He, F. Zhao, L. Huo, J. Mai, X. Lu, C.-J. Su, T. Li and J. Wang, *J. Am. Chem. Soc.* **2016**, *138*, 2973–2976.
- 19 F. Liu, Z. Zhou, C. Zhang, T. Vergote, H. Fan, F. Liu and X. Zhu, *J. Am. Chem. Soc.* **2016**, *138*, 15523–15526.
- 20 Y. Li, X. Liu, F.-P. Wu, Y. Zhou, Z.-Q. Jiang, B. Song, Y. Xia, Z.-G. Zhang, F. Gao and O. Inganäs, *J. Mater. Chem. A* **2016**, *4*, 5890–5897.
- 21 S. Holliday, R. S. Ashraf, A. Wadsworth, D. Baran, S. A. Yousaf, C. B. Nielsen, C.-H. Tan, S. D. Dimitrov, Z. Shang and N. Gasparini, *Nat. Commun.* **2016**, *7*, 11585–11595.
- 22 Z. Li, K. Jiang, G. Yang, J. Y. L. Lai, T. Ma, J. Zhao, W. Ma and H. Yan, *Nat. Commun.* **2016**, *7*, 13094–13102.
- 23 Y. Lin, J. Wang, Z. G. Zhang, H. Bai, Y. Li, D. Zhu and X. Zhan, *Adv. Mater.* **2015**, *27*, 1170–1174.
- 24 Z. Zheng, O. M. Awartani, B. Gautam, D. Liu, Y. Qin, W. Li, A. Bataller, K. Gundogdu, H. Ade and J. Hou, *Adv. Mater.* **2017**, *29*, 1604241–1604246.
- 25 L. Gao, Z. G. Zhang, H. Bin, L. Xue, Y. Yang, C. Wang, F. Liu, T. P. Russell and Y. Li, *Adv. Mater.* **2016**, *28*, 8288–8295.
- 26 H. Bin, Z.-G. Zhang, L. Gao, S. Chen, L. Zhong, L. Xue, C. Yang and Y. Li, *J. Am. Chem. Soc.* **2016**, *138*, 4657–4664.
- 27 Y. Yang, Z.-G. Zhang, H. Bin, S. Chen, L. Gao, L. Xue, C. Yang and Y. Li, *J. Am. Chem. Soc.* **2016**, *138*, 15011–15018.
- 28 C. B. Nielsen, S. Holliday, H.-Y. Chen, S. J. Cryer and I. McCulloch, *Acc. Chem. Res.* **2015**, *48*, 2803–2812.
- 29 Y. Lin and X. Zhan, *Adv. Energy Mater.* **2015**, *5*, 1501063.
- 30 H. Bai, Y. Wang, P. Cheng, Y. Li, D. Zhu and X. Zhan, *ACS Appl. Mater. Interfaces* **2014**, *6*, 8426–8433.
- 31 S.-L. Chang, F.-Y. Cao, W.-C. Huang, P.-K. Huang, C.-S. Hsu and Y.-J. Cheng, *ACS Appl. Mater. Interfaces* **2017**, *9*, 24797–24803.
- 32 W. Zhao, S. Li, H. Yao, S. Zhang, Y. Zhang, B. Yang and J. Hou, *J. Am. Chem. Soc.* **2017**, *139*, 7148–7151.
- 33 K. Cnops, G. Zango, J. Genoe, P. Heremans, M. V. Martinez-Diaz, T. Torres and D. Cheyns, *J. Am. Chem. Soc.* **2015**, *137*, 8991–8997.
- 34 S. Li, W. Liu, M. Shi, J. Mai, T.-K. Lau, J. Wan, X. Lu, C.-Z. Li and H. Chen, *Energy Environ. Sci.* **2016**, *9*, 604–610.
- 35 H. Lin, S. Chen, Z. Li, J. Y. L. Lai, G. Yang, T. McAfee, K. Jiang, Y. Li, Y. Liu and H. Hu, *Adv. Mater.* **2015**, *27*, 7299–7304.
- 36 F.-Y. Cao, W.-C. Huang, S.-L. Chang and Y.-J. Cheng, *Chem. Mater.* **2018**, *30*, 4968–4977.
- 37 S.-L. Chang, F.-Y. Cao, W.-C. Huang, P.-K. Huang, K.-H. Huang, C.-S. Hsu and Y.-J. Cheng, *ACS Energy Lett.* **2018**, *3*, 1722–1729.
- 38 J. Yuan, Y. Zhang, L. Zhou, G. Zhang, H.-L. Yip, T.-K. Lau, X. Lu, C. Zhu, H. Peng, P. A. Johnson, M. Leclerc, Y. Cao, J. Ulanski, Y. Li and Y. Zou, *Joule* **2019**, *3*, 1140–1151.
- 39 L. Hong, H. Yao, Z. Wu, Y. Cui, T. Zhang, Y. Xu, R. Yu, Q. Liao, B. Gao, K. Xian, H. Y. Woo, Z. Ge and J. Hou, *Adv. Mater.* **2019**, *31*, 1903441.
- 40 K. Li, Y. Wu, Y. Tang, M.-A. Pan, W. Ma, H. Fu, C. Zhan and J. Yao, *Adv. Energy Mater.* **2019**, *9*, 1901728.
- 41 Y. Lin, B. Adilbekova, Y. Firdaus, E. Yengel, H. Faber, M. Sajjad, X. Zheng, E. Yarali, A. Seitkhan, O. M. Bakr, A. El-Labban, U. Schwingenschlögl, V. Tung, I. McCulloch, F. Laquai and T. D. Anthopoulos, *Adv. Mater.* **2019**, *31*, 1902965.
- 42 S. Dai, F. Zhao, Q. Zhang, T.-K. Lau, T. Li, K. Liu, Q. Ling, C. Wang, X. Lu, W. You and X. Zhan, *J. Am. Chem. Soc.* **2017**, *139*, 1336–1343.
- 43 B. Jia, S. Dai, Z. Ke, C. Yan, W. Ma and X. Zhan, *Chem. Mater.* **2018**, *30*, 239–245.
- 44 N. Qiu, H. Zhang, X. Wan, C. Li, X. Ke, H. Feng, B. Kan, H. Zhang, Q. Zhang, Y. Lu and Y. Chen, *Adv. Mater.* **2017**, *29*, 1604964.
- 45 B. Kan, H. Feng, X. Wan, F. Liu, X. Ke, Y. Wang, Y. Wang, H. Zhang, C. Li, J. Hou and Y. Chen, *J. Am. Chem. Soc.* **2017**, *139*, 4929–4934.
- 46 W. Wang, C. Yan, T.-K. Lau, J. Wang, K. Liu, Y. Fan, X. Lu and X. Zhan, *Adv. Mater.* **2017**, *29*, 1701308.
- 47 T. Li, S. Dai, Z. Ke, L. Yang, J. Wang, C. Yan, W. Ma and X. Zhan, *Adv. Mater.* **2018**, *30*, 1705969.
- 48 S. Dai, T. Li, W. Wang, Y. Xiao, T.-K. Lau, Z. Li, K. Liu, X. Lu and X. Zhan, *Adv. Mater.* **2018**, *30*, 1706571.
- 49 H. Yao, Y. Chen, Y. Qin, R. Yu, Y. Cui, B. Yang, S. Li, K. Zhang and J. Hou, *Adv. Mater.* **2016**, *28*, 8283–8287.
- 50 F. Zhao, S. Dai, Y. Wu, Q. Zhang, J. Wang, L. Jiang, Q. Ling, Z. Wei, W. Ma, W. You, C. Wang and X. Zhan, *Adv. Mater.* **2017**, *29*, 1700144.
- 51 S. Li, L. Ye, W. Zhao, S. Zhang, S. Mukherjee, H. Ade and J. Hou, *Adv. Mater.* **2016**, *28*, 9423–9429.
- 52 Z. Luo, H. Bin, T. Liu, Z.-G. Zhang, Y. Yang, C. Zhong, B. Qiu, G. Li, W. Gao, D. Xie, K. Wu, Y. Sun, F. Liu, Y. Li and C. Yang, *Adv. Mater.* **2018**, *30*, 1706124.
- 53 D. Baran, R. S. Ashraf, D. A. Hanifi, M. Abdelsamie, N. Gasparini, J. A. Röhr, S. Holliday, A. Wadsworth, S. Lockett, M. Neophytou, C. J. M. Emmott, J. Nelson, C. J. Brabec, A. Amassian, A. Salleo, T. Kirchartz, J. R. Durrant and I. McCulloch, *Nat. Mater.* **2016**, *16*, 363.
- 54 H. Yao, L. Ye, J. Hou, B. Jang, G. Han, Y. Cui, G. M. Su, C. Wang, B. Gao, R. Yu, H. Zhang, Y. Yi, H. Y. Woo, H. Ade and J. Hou, *Adv. Mater.* **2017**, *29*, 1700254.
- 55 S.-L. Chang, K.-E. Hung, F.-Y. Cao, K.-H. Huang, C.-S. Hsu, C.-Y. Liao, C.-H. Lee and Y.-J. Cheng, *ACS Appl. Mater. Interfaces* **2019**, *11*, 33179–33187.
- 56 Y. Lin, F. Zhao, Q. He, L. Huo, Y. Wu, T. C. Parker, W. Ma, Y. Sun, C. Wang, D. Zhu, A. J. Heeger, S. R. Marder and X. Zhan, *J. Am. Chem. Soc.* **2016**, *138*, 4955–4961.
- 57 Z. Fei, F. D. Eisner, X. Jiao, M. Azzouzi, J. A. Röhr, Y. Han, M. Shahid, A. S. R. Chesman, C. D. Easton, C. R. McNeill, T. D. Anthopoulos, J. Nelson and M. Heeney, *Adv. Mater.* **2018**, *30*, 1705209.
- 58 H. Lu, J. Zhang, J. Chen, Q. Liu, X. Gong, S. Feng, X. Xu, W. Ma and Z. Bo, *Adv. Mater.* **2016**, *28*, 9559–9566.
- 59 J. Wang, W. Wang, X. Wang, Y. Wu, Q. Zhang, C. Yan, W. Ma, W. You and X. Zhan, *Adv. Mater.* **2017**, *29*, 1702125.
- 60 Y. Liu, C. e. Zhang, D. Hao, Z. Zhang, L. Wu, M. Li, S. Feng, X. Xu, F. Liu and X. Chen, *Chem. Mater.* **2018**, *30*, 4307–4312.
- 61 H. Huang, L. Yang, A. Facchetti and T. J. Marks, *Chem. Rev.* **2017**, *117*, 10291–10318.
- 62 S. W. Kim, Y. J. Lee, Y. W. Lee, C. W. Koh, Y. Lee, M. J. Kim, K. Liao, J. H. Cho, B. J. Kim and H. Y. Woo, *ACS Appl. Mater. Interfaces* **2018**, *10*, 39952–39961.

- 63 Y. Liu, Z. Zhang, S. Feng, M. Li, L. Wu, R. Hou, X. Xu, X. Chen and Z. Bo, *J. Am. Chem. Soc.*, **2017**, *139*, 3356-3359.
- 64 X. Shi, X. Liao, K. Gao, L. Zuo, J. Chen, J. Zhao, F. Liu, Y. Chen and A. K. Y. Jen, *Adv. Funct. Mater.*, **2018**, *28*, 1802324.
- 65 S. Dai, Y. Xiao, P. Xue, J. James Rech, K. Liu, Z. Li, X. Lu, W. You and X. Zhan, *Chem. Mater.*, **2018**, *30*, 5390-5396.
- 66 X. Shi, L. Zuo, S. B. Jo, K. Gao, F. Lin, F. Liu and A. K. Y. Jen, *Chem. Mater.* **2017**, *29*, 8369-8376.
- 67 L. Zuo, X. Shi, S. B. Jo, Y. Liu, F. Lin and A. K. Y. Jen, *Adv. Mater.* **2018**, *30*, 1706816.
- 68 Y. Li, K. Yao, H. L. Yip, F. Z. Ding, Y. X. Xu, X. Li, Y. Chen and A. K. Y. Jen, *Adv. Funct. Mater.* **2014**, *24*, 3631-3638.
- 69 F.-Y. Cao, P.-K. Huang, Y.-C. Su, W.-C. Huang, S.-L. Chang, K.-E. Hung and Y.-J. Cheng, *J. Mater. Chem. A*, **2019**, *7*, 17947-17953.
- 70 S. Feng, D. Ma, L. Wu, Y. Liu, C. e. Zhang, X. Xu, X. Chen, S. Yan and Z. Bo, *Sci China Chem*, **2018**, *61*, 1320-1327.
- 71 B. Gao, H. Yao, B. Jang, J. Zhu, R. Yu, Y. Cui, F. Wang, J. Hou, H. Y. Woo and J. Hou, *J. Mater. Chem. A*, **2018**, *6*, 2664-2670.
- 72 J. Wang, J. Zhang, Y. Xiao, T. Xiao, R. Zhu, C. Yan, Y. Fu, G. Lu, X. Lu, S. R. Marder and X. Zhan, *J. Am. Chem. Soc.*, **2018**, *140*, 9140-9147.
- 73 W. Zhong, J. Cui, B. Fan, L. Ying, Y. Wang, X. Wang, G. Zhang, X.-F. Jiang, F. Huang and Y. Cao, *Chem. Mater.* **2017**, *29*, 8177-8186.
- 74 Y.-C. Lin, Y.-W. Su, J.-X. Li, B.-H. Lin, C.-H. Chen, H.-C. Chen, K.-H. Wu, Y. Yang and K.-H. Wei, *J. Mater. Chem. A*, **2017**, *5*, 18053-18063.
- 75 T. Zhang, X. Zhao, D. Yang, Y. Tian and X. Yang, *Adv. Energy Mater.* **2018**, *8*, 1701691-1701699.
- 76 W. Lee, J.-H. Kim, T. Kim, S. Kim, C. Lee, J.-S. Kim, H. Ahn, T.-S. Kim and B. J. Kim, *J. Mater. Chem. A* **2018**, *6*, 4494-4503.
- 77 T. Kim, J. Choi, H. J. Kim, W. Lee and B. J. Kim, *Macromolecules* **2017**, *50*, 6861-6871.
- 78 D. Veldman, S. C. Meskers and R. A. Janssen, *Adv. Funct. Mater.*, **2009**, *19*, 1939-1948.
- 79 S. Chen, Y. Liu, L. Zhang, P. C. Chow, Z. Wang, G. Zhang, W. Ma and H. Yan, *J. Am. Chem. Soc.*, **2017**, *139*, 6298-6301.

View Article Online
DOI: 10.1039/C9TA14040A

Table of contents

TT-terminal ladder-type donor is generally a better molecular design than the corresponding T-terminal ladder-type isomer for development of new A-D-A FREAs.

